FEMS Yeast Research, 2024, **24**, foae024
DOI: 10.1093/femsyr/foae024
Advance access publication date: 5 August 2024
Research Article

Exploring yeast biodiversity and process conditions for optimizing ethylene glycol conversion into glycolic acid

Vittorio Giorgio Senatore, Riccardo Milanesi, Fiorella Masotti, Letizia Maestroni, Stefania Pagliari, Ciro Cannavacciuolo, Luca Campone, Immacolata Serra, Paola Branduardi*

Department of Biotechnology and Biosciences, University of Milano-Bicocca, Piazza della Scienza 2, 20126 Milan, Italy
*Corresponding author. Department of Biotechnology and Biosciences, University of Milano-Bicocca, Piazza della Scienza 2, 20126, Milan, Italy. E-mail: paola.branduardi@unimib.it
Editor: [John Morrissey]

Abstract

Plastics have become an indispensable material in many fields of human activities, with production increasing every year; however, most of the plastic waste is still incinerated or landfilled, and only 10% of the new plastic is recycled even once. Among all plastics, polyethylene terephthalate (PET) is the most produced polyester worldwide; ethylene glycol (EG) is one of the two monomers released by the biorecycling of PET. While most research focuses on bacterial EG metabolism, this work reports the ability of *Saccharomyces cerevisiae* and nine other common laboratory yeast species not only to consume EG, but also to produce glycolic acid (GA) as the main by-product. A two-step bioconversion of EG to GA by *S. cerevisiae* was optimized by a design of experiment approach, obtaining 4.51 ± 0.12 g l^{-1} of GA with a conversion of $94.25 \pm 1.74\%$ from 6.21 ± 0.04 g l^{-1} EG. To improve the titer, screening of yeast biodiversity identified *Scheffersomyces stipitis* as the best GA producer, obtaining 23.79 ± 1.19 g l^{-1} of GA (yield 76.68%) in bioreactor fermentation, with a single-step bioprocess. Our findings contribute in laying the ground for EG upcycling strategies with yeasts.

Keywords: *Saccharomyces cerevisiae*; *Scheffersomyces stipitis*; glycolic acid; ethylene glycol; biodiversity; polyethylene terephthalate

Introduction

Since the first synthetic polymer development in 1907, plastics have become an everyday necessity in almost every aspect of our life. Indeed, plastics have unique properties such as strength, water resistance, and durability (Amalia et al. 2024) that make them exceptional for a wide variety of applications. Almost 400 Mt of new plastics were produced in 2020, and it is estimated that the production will reach 1000 Mt by 2050 (Hundertmark et al. 2018). However, the properties that make plastic so widespread are the very same ones that make plastic recycling incredibly difficult. As an example, in 2020, less than 10% of the newly produced plastics was recycled even once, and less than 1% was recycled twice (Tiso et al. 2022). Incineration (42%), landfilling (19%), and export (10%) are the most common fates of postconsumer plastic waste; about 9% is dispersed or enters the environment due to waste mismanagement; overall, only 20% of postconsumer plastic waste was recycled in 2016 (Orlando et al. 2023). Recycling remains a complex process, requiring sorting, processing, and physical–chemical treatments that ultimately results in a lower quality product (Lee et al. 2023).

Among all plastics, polyethylene terephthalate (PET) is the most abundant polyester produced worldwide (Soong et al. 2022) and it is one of the most used commodity plastics (Amalia et al. 2024). PET is a thermoplastic polymer obtained from the polycondensation of terephthalic acid (TPA) and ethylene glycol (EG), both mostly obtained from nonrenewable resources (Ren et al. 2024). It is widely used in the manufacturing of water bottles, food packaging, and textiles thanks to its ability to withstand high temperatures, and its resistance to chemical and physical degradation (Muringayil Joseph et al. 2024).

The majority of waste PET is landfilled, incinerated, or dispersed in the environment; only about 30% is recycled, mostly by mechanical methods which create PET flakes to be melted in new products, generally with worse characteristics with respect to virgin PET (Muringayil Joseph et al. 2024, Ren et al. 2024). Enzymatic recycling (or biorecycling) is an emerging strategy for PET depolymerization, employing enzymes to break down products into their monomers; the most studied enzymatic activities include PETases, cutinases, lipases, and carboxylesterases (Weiland et al. 2024). This approach is still in its early stages, however the French company Carbios is proving the feasibility of this approach and it is currently building a biorecycling plant with a 50k tons PET feedstock capacity to produce monomers of virgin-like quality (Tournier et al. 2020, Carbios 2024). Several studies have been focusing on the upcycling of the monomers into more valuable commodity chemicals to enhance the economic viability of enzymatic recycling (Lee et al. 2023, Amalia et al. 2024); such an example is the upcycling of EG to glycolic acid (GA).

GA is a small two-carbon α-hydroxy acid with a widespread application in various industries, such as personal care, pharmaceuticals, medical, and textiles (Salusjärvi et al. 2019). The global GA market size is growing and it is expected to reach USD 565.3 million by 2030, registering a CAGR of 9.1% from 2023 to 2030, with the personal care segment holding the largest revenue share (61.1%) in 2022 (https://www.grandviewresearch.com/press-release/global-glycolic-acid-market; accessed 25 April 2024). GA is currently produced chemically from petrochemical

Received 17 June 2024; **revised** 26 July 2024; **accepted** 2 August 2024

resources, due to the relatively high price of EG (Salusjärvi et al. 2019). However, with EG from waste PET becoming more available, different strategies for the microbial production of GA from EG have been proposed (Kataoka et al. 2001, Deng et al. 2018, Hua et al. 2018, Cabulong et al. 2019, Carniel et al. 2023, Yu et al. 2023).

Two main EG assimilation pathways have been identified. In aerobic bacteria (*Pseudomonas* spp., *Escherichia coli*), EG is oxidized to glycolaldehyde (GAH) and then to GA; GA is incorporated in the central carbon metabolism by further oxidation to glyoxylate (GOX) and condensation to tartronate semialdehyde (Gao et al. 2022). In the anaerobic acetogenic bacterium *Acetobacterium woodii*, EG is dehydrated to acetaldehyde and then disproportionated to ethanol and acetate; unfortunately, the dehydratase is very oxygen-sensitive (Trifunović et al. 2016, Levin and Balskus 2018). Some bacterial species, on the other hand, are able to metabolize EG only up to GA. This is the case for the most studied GA producer *Gluconobacter oxydans*, which is able to catalyse the oxidation of EG to GAH with Gox0313, a NAD^+-dependent alcohol dehydrogenase (Zhang et al. 2015). To the best of our knowledge, EG oxidation to GA has been reported in yeast only by two works, still the pathway remains putative, most likely involving nonspecific dehydrogenases (Kataoka et al. 2001, Carniel et al. 2023). No hypotheses on assimilation are present.

This work aims to lay the ground for the physiology of EG metabolism in yeast, focusing on the well-known *Saccharomyces cerevisiae* and nine other different yeasts. *S. cerevisiae*'s ability to metabolize EG was first investigated during growth in the presence of glucose; secondly, a two-step bioconversion of EG to GA was optimized by a design of experiment (DoE) approach, to understand the determining process parameters. Despite the optimization, EG consumption remains limited in *S. cerevisiae*, thus to improve the process performance nine non-*Saccharomyces* yeasts were screened for high EG consumption with high GA production. This ultimately allowed the design of a single-step bioprocess in 2 l bioreactors with the best producer. By design, the developed process does not rely on offline data for monitoring, thus avoiding the need of specialized instruments and personnel to assess the quality of the fermentation.

The physiological data obtained in this work will pave the way for further genetic and metabolic studies to improve EG conversion to GA and to discover the genes involved in the pathway.

Materials and methods

Strains and media composition

Saccharomyces cerevisiae CEN.PK 113–7D, *Cutaneotrichosporon oleaginosus* (ATCC 20509, previously known as *Trichosporon oleaginosus*), *Cryptococcus oleaginosus* (DSM 70022, previously known as *Cryptococcus curvatus*), *Kluyveromyces lactis* (CBS2359), *Kluyveromyces marxianus* (NBRC1777), *Komagataella phaffii* X-33 (Invitrogen), *Rhodotorula toruloides* (DSM 4444), *Scheffersomyces stipitis* (CBS 6054), *Zygosaccharomyces bailii* (ATCC 8766), and *Zygosaccharomyces parabailii* (ATCC 60483) were maintained in 20% (v/v) glycerol at −80°C after growth in YPD medium composed of (per liter): yeast extract 10 g, tryptone 20 g, and glucose 20 g.

YP medium was composed of (per liter): yeast extract 10 g, tryptone 20 g. Unless differently specified, EG was added to a final concentration of 150 mM (9.3 g l^{-1}).

Yeast extract was purchased from Biolife Italia S.r.l., Milan, Italy. All other reagents were purchased from Merk Life Science S.r.l., Milan, Italy.

Growth conditions for each experiment are described below and summarized in Table S1.

Growth conditions in 96-well microplate for EG toxicity assessment

To test EG toxicity, *S. cerevisiae* was grown in 96-well plates (flat bottom) on YPD with increasing concentrations of EG (0, 3, 12, 48, 100, and 150 mM, corresponding to 0, 0.2, 0.8, 3, 6.2, and 9.3 g l^{-1}) at pH 3.0, 3.5, 4.0, and 5.0; all combinations of EG concentrations and pH were tested; HCl 1 M was used to reach the desired pH.

Seed cultures from YPD plates were grown in glass tubes filled with 2 ml YPD for 8 h; cells were then inoculated for the intermediate inoculum (starting OD = 0.01) in 50 ml glass tubes containing 10 ml of YPD, and grown for 16 h. Cells were then harvested, washed with dH_2O and inoculated in the microplate wells (final OD = 0.5, calculated in a cuvette with a light path of 1 cm) each filled with 200 µl of medium. Growth was performed at 30°C under constant agitation (1000 rpm) in a microplate shaker.

Growth was monitored every 1 h during the exponential phase using a multiscan spectrophotometer set at 600 nm (VICTOR™ X3, PerkinElmer). Growth rate was estimated by fitting a regression line on the logarithm of the OD measurements; the slope of the line was used to represent the growth rate.

Growth conditions in shake flasks

Growth conditions in 250 ml shake flasks with S. cerevisiae

EG metabolism in the presence of glucose was studied with *S. cerevisiae* in 250 ml shake flasks, in YPD + EG medium.

Seed cultures from YPD plates were grown in glass tubes filled with 2 ml YPD for 8 h; cells were then inoculated for the intermediate inoculum (starting OD = 0.01) in 50 ml glass tubes containing 10 ml of YPD, and grown for 16 h. Cells were then harvested, washed with dH_2O and inoculated in shake flasks (final OD = 0.5) filled with 50 ml of medium under investigation. All growths were performed in a rotary shaker at 160 rpm and 30°C. Samples were collected at regular time intervals for OD and HPLC analysis.

Growth conditions in 100 ml shake flasks for the screening with non-Saccharomyces yeasts

The ability to oxidize EG to GA of non-*Saccharomyces* yeasts was assayed in 100 ml shake flasks, in YP + EG medium; *S. cerevisiae* was assayed as a reference condition.

Seed cultures from YPD plates were grown in 50 ml glass tubes filled with 10 ml YP for 24 h; cells were then harvested, washed with dH_2O and inoculated in shake flasks (final OD = 1.0) filled with 20 ml of YP + EG. The higher initial cell density was chosen considering the fact that not all yeast species (*S. cerevisiae* being an example) are able to grow efficiently on YP. All growths were performed in a rotary shaker at 160 rpm and 30°C. Samples were collected at regular time intervals for OD measurement and HPLC analysis. Two independent replicates were performed for each strain.

Two-step bioconversion approach: optimization by DoE

Growth conditions in batch bioreactor for biomass accumulation

Saccharomyces cerevisiae biomass was grown in 2 l stirred-tank bioreactors (BIOSTAT® A plus, Sartorius Stedim Biotech GmbH, Goettingen, Germany) equipped with Visiferm DO ECS 225 for pO_2 measurement and Easyferm Plus K8 200 for pH measurement (both from Hamilton Bonaduz AG, Bonaduz, Switzerland), with a

working volume of 1 l. The temperature was kept constant at 30°C and pH was set to 5.5, maintained by automatic addition of 2 M KOH and 1 M HCl. The stirring rate was set to 300 rpm in cascade to maintain the oxygen concentration, which was set to 25% of saturation, to guarantee a completely aerobic condition to the cell culture. Filtered air (pore size 0.2 µm) was continuously sparged through the reactor at a flow rate of 1 vvm. Foam formation was controlled by the addition of polypropylene glycol (PPG) at a concentration of 1 ml l^{-1}.

Seed cultures from YPD plates were grown for 8 h in glass tubes in 10 ml YPD; cells were then inoculated for the intermediate inoculum (starting OD = 0.05) in 250 ml shake flasks containing 50 ml of YPD and grown overnight (16 h). The preinocula were performed in a rotary shaker at 160 rpm and 30°C. For the inoculum, cells were harvested, washed with sterile dH_2O, and used to inoculate the bioreactor (starting OD = 0.5).

Cells in exponential phase were harvested after 8 h of cultivation; cells in stationary phase were harvested after 48 h of cultivation; online data combined with HPLC analysis was used to determine the time of harvest. Prior to inoculation for the bioconversion experiments, cells were washed twice with dH_2O.

Experimental design

Chemometric approach was used to find the best bioconversion parameters using Statgraphic Centurion XVI 16.1 version (Rockville, USA.).

For a first screening of the variables (Round 1), a Folded Plackett–Burman with an error of 14 degrees of freedom, for a total of 24 randomized runs was used (Table S2). Nine experimental factors were studied: shaking (160–280 rpm), growth phase (exponential or stationary), medium (100 mM potassium phosphate buffer or YP), pH (6–8), EG concentration (20–100 mM), volume of medium to volume of flask ration (m/f ratio) (5–15), flask type (regular or baffled), biomass (10–50 OD ml^{-1}), and time (1–7 days). Shaking, m/f ratio and flask type were chosen to study the influence of oxygenation and mass transfer. The amount of time, biomass and the growth phase at which cells were collected were chosen to study the influence of these factors on process efficiency and productivity: fewer cells require less substrate to obtain the biomass and cells in exponential phase allow a shorter biomass production phase (8 h versus 72 h). Medium was chosen to evaluate the possibility to use a buffer of known composition (as opposed to YP) to make a potential purification step more straight-forward. EG concentration and pH were chosen to study whether the bioconversion would benefit from a lower starting EG concentration and if maintenance of an adequate pH (acid or basic) was fundamental for the process. GA concentration (g l^{-1}) and molar conversion of consumed EG to GA (% mol mol^{-1}) were used as response variables. Table S2 reports the experimental matrix design of Round 1, with the experimental levels of the independent variables (factors) and the results obtained for the analysed response variables. Results from the bioconversion experiments were subjected to regression analysis using linear regression methodology to obtain the parameters of the mathematical models. Analysis of variance (ANOVA) was applied to evaluate the statistical significance of independent variable contributions and their first order interaction. The effect of each factor on the response variables was analysed from the standardized Pareto chart and a first mathematical model was obtained. The extrapolated optimized conditions were as follows: shaking (280 rpm), growth phase (stationary), medium (YP), pH (8), EG concentration (100 mM), m/f ratio (15), flask type (baffled), biomass (50 OD ml^{-1}), and time (7 days), with shaking, growth phase, medium, and pH having a P-value < 0.05.

From this first screening, a new experimental design (Round 2) was set up. Growth phase (stationary), EG concentration (100 mM), m/f ratio (15), flask type (baffled), biomass (50 OD ml^{-1}), and time (7 days) were fixed, and a Box–Behnken design with four center points, an error of 6 degrees of freedom, for a total of 16 randomized runs was used (Table 1). Three experimental factors were studied: shaking (220, 250, or 280 rpm), YP dilution (1:1, 1:3, and 1:5), potassium phosphate buffer pH 8 concentration (100, 200, and 300 mM). GA concentration (g l^{-1}) and molar conversion of consumed EG to GA (% mol mol^{-1}) were used as response variables. Table 1 reports the experimental matrix design of Round 2, with the experimental levels of the independent variables (factors) and the results obtained for the analysed response variables. Results from the bioconversion experiments were subjected to regression analysis using least squares regression methodology to obtain the parameters of the mathematical model. ANOVA was applied to evaluate the statistical significance of independent variable contributions and their first order interaction. The effect of each factor on the response variables was analysed from the standardized Pareto chart, and response surfaces of the mathematical models were obtained. Finally, the optimized conditions extrapolated by Box–Behnken design were as follows: shaking (280 rpm), YP dilution (1:1), buffer concentration (100 mM), with only shaking having a P-value < 0.05.

Growth conditions in 6-deepwell microplates

Bioconversion of EG to GA by *S. stipitis* and *C. oleaginosus* ATCC 20509 was assayed more in detail in 6-deepwell microplates (CR1406, manufactured by Enzyscreen, Heemstede, The Netherlands), providing better mixing and aeration than traditional shake flasks. Bioconversion was performed in buffered YP + EG medium pH 7; the buffer used was 100 mM potassium hydrogen phthalate. Control conditions were performed without adding EG to the growth medium.

Seed cultures from YPD plates were grown in glass tubes filled with 2 ml YPD for 8 h; cells were then inoculated for the intermediate inoculum (starting OD = 0.1) in 50 ml glass tubes containing 10 ml of YPD, and grown for 16 h. Cells were then harvested, washed with dH_2O and inoculated in the 6-deepwell microplate wells (final OD = 0.5) each filled with 30 ml of medium under investigation. All growths were performed in a rotary shaker (19 mm stroke) at 300 rpm and 30°C (as per manufacturer indications). Samples were collected at regular time intervals for OD and pH measurement, and HPLC analysis.

Growth rate was estimated by fitting a regression line on the logarithm of the OD measurements; the slope of the line was used to represent the growth rate.

Production of GA in 2 l bioreactors

Growth conditions in bioreactor

Scheffersomyces stipitis was grown in 2 l stirred tank bioreactors (BIOSTAT® A plus, Sartorius Stedim Biotech GmbH) equipped with Visiferm DO ECS 225 for pO_2 measurement and Easyferm Plus K8 200 for pH measurement (both from Hamilton Bonaduz AG) with a working volume of 800 ml. The temperature was kept constant at 30°C and pH was set to 6.0, maintained by automatic addition of 2 M KOH and 1 M HCl. The stirring rate was set to 300 rpm in cascade to maintain the oxygen concentration, which was set to 25% of saturation, to guarantee a completely aerobic condition to the cell culture. Filtered air (pore size 0.2 µm) was continuously

Table 1. Experimental conditions of the response surface design (Box–Behnken) and experimental values of the response variables for Round 2. Values are the mean of three independent experiments.

	Independent variables			Response variables	
Run	Shaking (rpm)	YP dilution	Buffer concentration (mM)	[GA] (g l^{-1})	Conversion (% mol mol^{-1})
1	220	1:5	200	2.17	55.02
2	250	1:1	300	3.15	57.41
3	280	1:3	100	4.46	67.51
4	250	1:5	100	3.23	57.95
5	280	1:1	200	4.95	79.63
6	250	1:3	200	3.51	57.62
7	250	1:1	100	3.93	71.25
8	220	1:3	300	4.17	57.78
9	250	1:5	300	3.54	59.05
10	250	1:3	200	3.54	58.76
11	280	1:5	200	4.84	66.30
12	250	1:3	200	3.29	55.55
13	220	1:3	100	2.74	35.42
14	250	1:3	200	4.11	61.47
15	220	1:1	200	2.34	60.23
16	280	1:3	300	4.32	69.67

sparged through the reactor at a flow rate of 1–4 vvm. Foam formation was controlled by the addition of PPG at a concentration of 1 ml l^{-1}. Gas analysers (BlueVery, BlueSens gas sensor GmbH) were attached to the outgas for online measurement of $\%CO_2$ and $\%O_2$ in the air.

Seed cultures from YPD plates were grown for 8 h in glass tubes in 10 ml YPD; cells were then inoculated for the intermediate inoculum (starting OD 0.05) in 250 ml baffled shake flasks containing 50 ml of YPD and grown overnight (16 h). The preinocula were performed in a rotary shaker at 250 rpm and 30°C. For the inoculum, cells were harvested, washed with sterile dH_2O, and used to inoculate the bioreactor (starting OD = 0.5).

The medium for the production was YPD40 medium composed of (per liter): yeast extract 10 g, tryptone 20 g, and glucose 40 g. After the exhaustion of glucose and the YP nutrients (at 24 h), a pulse of EG (11 ml, corresponding to 200 mmol, corresponding to a concentration of about 250 mM) was performed and GA production monitoring started. Samples were collected at regular time intervals for OD and cell dry weight (CDW) measurement, and HPLC analysis. Two independent replicates were performed.

Downstream processing

After the fermentation was stopped (144 h), the fermentation broth was pelleted at 4000 × *g* for 1 h at 4°C; the supernatant was filter-sterilized for storage at 4°C.

Online process monitoring

Consumption of glucose can be indirectly monitored by the pO_2 profile and by the online $\%CO_2$ in the outgas; thus, the time of addition of EG is easy to determine, as no offline measurements (e.g. HPLC) are required. Moreover, the production of GA (and thus the consumption of EG) can be followed by the addition of KOH to maintain the desired pH; as the concentration of base is known, as well as how much volume of base is added at any time, the total amount of GA produced can be easily estimated (1 mol of base = 1 mol of GA) with Eq. (1) as follows:

$$GA_{ti} \approx (KOH_{ti} - KOH_{EG}) \cdot 10^{-3}\ [l] \cdot 2\ [\text{mol}\ l^{-1}] \cdot 76.05\ [\text{g}\ \text{mol}^{-1}], \quad (1)$$

where GA_{ti} is the estimated quantity of GA in grams at time t_i, KOH_{ti} and KOH_{EG} are the volumes of KOH added at time t_i and at the time of the EG pulse (in ml), respectively, 2 mol l^{-1} is the concentration of KOH, and 76.06 g mol^{-1} is the molecular weight of GA. The general assumption is that GA is the only acid produced in this phase, and thus the moles of added KOH correspond to the moles of GA produced.

Calculation of fermentation parameters

Yield of EG conversion to GA was calculated as the ratio of the moles of GA at the end of the fermentation and the moles of EG; the maximum yield is 100%, as one mole of EG can at most be converted to one mole of GA.

Metabolites quantification by HPLC

HPLC analysis was performed to quantify the amount of glucose, EG and GA; production of fermentation by-products such as ethanol, acetate, and glycerol was also monitored. Prior to analysis, all samples were centrifuged (21 000 × *g*, 5') and diluted when necessary. The HPLC was equipped with a Rezex ROA-Organic Acid H^+ (8%) Ion Exclusion column 300 mm × 7.8 mm, 8 µm (Phenomenex); 10 µl of samples were injected in the column. The mobile phase was H_2SO_4 0.005 N, at a flow of 0.8 ml min^{-1}; column temperature was set to 80°C. Separated components were detected by a refractive index detector, and by a variable wavelength detector set at 210 nm. Peaks were identified by comparison with reference standards dissolved in ultrapure H_2O (18 MΩ). Calibration curves for peak quantification were prepared in a range between 0.625 and 40.0 g l^{-1}.

Statistical analysis

Unless differently stated, the experiments were performed with three independent replicates. GraphPad PRISM 10.1.0 was used for the statistical analysis of fermentation parameters. For the toxicity test, a two-way ANOVA was performed to analyse the effect of EG concentration and growth medium pH on growth rate, followed by a *post hoc* Tukey–Kramer test for multiple comparisons. The remaining statistical analyses were performed using a two-tailed, unpaired, heteroscedastic Student's *t*-test.

Results and discussion

EG toxicity test and native metabolism in *S. cerevisiae*

With the aim to investigate EG metabolism with *S. cerevisiae*, an assessment on EG toxicity and its metabolism was required, as to the best of our knowledge, such information is not available in the scientific literature regarding this yeast.

First, EG toxicity was evaluated by growing *S. cerevisiae* in 96-wells microplates and by measuring differences in the growth rate (Fig. S1). To sample the toxicity around low concentrations of EG, the interval 0–150 mM was divided into six intervals using a logarithmic scale; at the same time, the effect of pH was evaluated, too. The range of EG concentrations was selected by taking into account that PET might be the source of EG: if this were the case, a release of 150 mM EG (9.3 g l^{-1}) would correspond to a similar TPA concentration (150 mM, 25 g l^{-1}). In terms of weak organic stress, 150 mM is a high amount, thus we decided to limit our study to this concentration, despite some yeast species are reported to tolerate much higher EG concentrations (Kataoka et al. 2001, Carniel et al. 2023). Figure S1 shows the growth rates in the 24 conditions tested and OD raw data for each condition. Statistical results from the ANOVA analysis on the measured growth rates showed no significant differences in the class "[EG]", while it did show a *P*-value < .05 for the class pH (which is expected, but independently from EG presence). Multiple comparisons between each condition couple showed no significant difference. From these results, we concluded that EG is not toxic for *S. cerevisiae* in the tested conditions and concentrations, and therefore 150 mM EG was used in the following experiments. Nonetheless, a recent investigation showed that *Yarrowia lipolytic a* can tolerate up to 2 M EG (Carniel et al. 2023), suggesting that *S. cerevisiae* tolerance might be actually higher than 150 mM.

As HPLC analysis of the supernatants at 48 h showed a decrease in the concentration of EG (data not shown), we decided to better characterize the EG metabolism of *S. cerevisiae* in the presence of glucose. Thus, we grew *S. cerevisiae* in YPD + EG to understand when EG uptake happens and if by-products (GA, specifically) are produced (Fig. 1). Indeed, *S. cerevisiae* is able to consume EG and to produce GA as a by-product. Most importantly, EG consumption only starts after the depletion of all the other carbon sources (glucose, acetate, and ethanol), in a very late stage of the fermentation process. No differences of fermentation profiles were observed with the control condition, where EG was not provided in the growth medium (data not shown). A very similar behavior was observed in buffered defined minimal medium (Delft; Verduyn et al. 1992) with 150 mM EG (data not shown).

To the best of our knowledge, EG metabolism in yeasts has not been described in detail. Few works are available in literature regarding EG transformation by yeasts and the majority of the studies focuses on *Y. lipolytica* (Kataoka et al. 2001, Da Costa et al. 2020, Kosiorowska et al. 2022a, 2022b, Sales et al. 2022, 2023, Carniel et al. 2023). Both Da Costa et al. (2020) and Kosiorowska et al. (2022b) reported that *Y. lipolytica* (strain IMUFRJ 50682 and a strain derived from the A101 strain, respectively) is able to coconsume EG with glucose in rich medium (YPD); however, no mention of by-product(s) is present. *Saccharomyces cerevisiae*, however, seems to behave differently. Moreover, in the latest work of Kosiorowska et al. (2022b), EG seems to strongly reduce glucose uptake rate; however, no explanation for the behavior is hypothesized. This is in contrast with the results obtained with *S. cerevisiae*, where

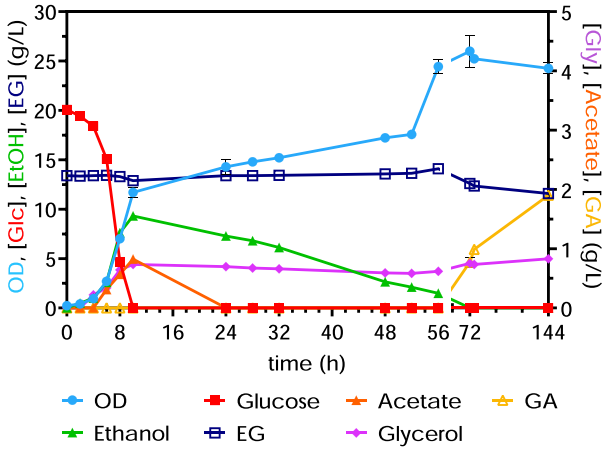

Figure 1. Growth of *S. cerevisiae* on YPD + EG. The figure shows the fermentation profile of *S. cerevisiae* on YPD + EG in 250 ml shake flasks. The left *y*-axis shows OD (blue, circles), and glucose (red, squares), ethanol (green, triangles), and EG (dark blue, hollow squares) concentration in g l^{-1}; the right *y*-axis shows glycerol (pink, diamonds), acetate (orange, triangles), and GA (yellow, hollow triangles) concentration in g l^{-1}. Values are the mean ± standard deviation of three independent experiments.

the presence of EG does not affect growth rate and glucose consumption, as described by the abovementioned results (Fig. 1). It is worth mentioning that in the most recent study listed above, Carniel et al. (2023) reported GA production from EG in *Y. lipolytica* IMUFRJ 50682, hypothesizing the contribution of endogenous alcohol and aldehyde dehydrogenases.

Taken together, our results suggest that the conversion of EG by *S. cerevisiae* is also very likely due to the activity of promiscuous enzymes, most probably dehydrogenases, possibly upregulated in the stationary phase. Based on the available literature, we propose the following EG oxidation pathway, outlined in Fig. 2. The first reaction might be catalysed by *YLL056C*, a NADH-dependent aldehyde reductase, which catalyses the oxidation of EG to GAH; the reaction; however, is favored toward the formation of EG (Wang et al. 2017). Other proteins were reported to be active on GAH, such as the products of genes *ADH1* (Jayakody et al. 2013), *GRE2* (Jayakody et al. 2018, Jayakody and Jin 2021), and others (*ADH7*, *SFA1*, *YML131W*, *YNL134C*, and *YKL107W*) (Jayakody et al. 2013, Jayakody and Jin 2021, Wang et al. 2019); however, no information on the directionality of the reaction toward the formation of the aldehyde is generally mentioned, as these works focus on GAH detoxification. Indeed, these aldehyde reductases are involved in aldehyde stress response, while *YLL056C* role still has not been elucidated. The subsequent oxidation of GAH to GA is reported to be catalysed by *ALD2*, *ALD3*, *ALD4*, and *ALD5* (metacyc.org). *ALD2* and *ALD3* encode two cytoplasmic stress-inducible isoforms, and are induced by a variety of stresses, among which oxidative stress and glucose exhaustion; *ALD4* and *ALD5* encode the mitochondrial isoforms. In the case of this oxidation reaction, the equilibrium is favored toward the formation of GA, rather than towards the reduction of GA to GAH.

All the reported genes are expressed in stress/limiting conditions, which is consistent with our observations: EG starts being consumed only after the exhaustion of the carbon sources in the growth medium (glucose, acetate, and ethanol). Further studies, however, are needed to confirm the suggested pathway.

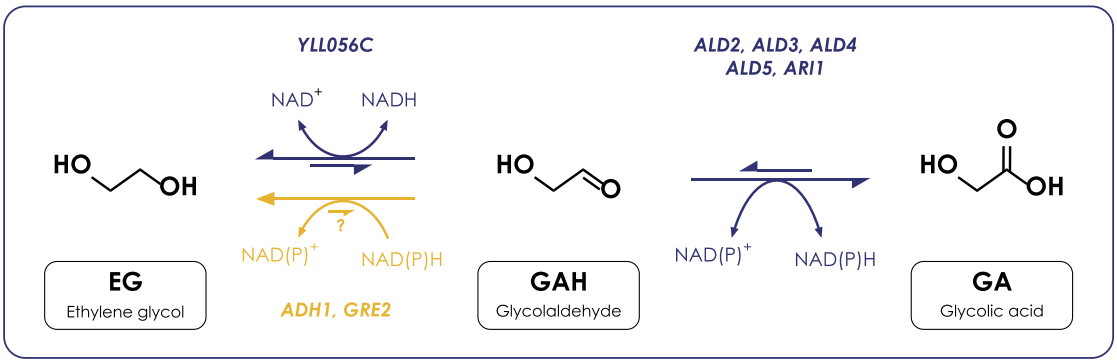

Figure 2. Proposed pathway for the oxidation of EG to GA in *S. cerevisiae*. EG is first oxidized to GAH by *YLL056C*, using NAD^+ as cofactor; the reaction equilibrium; however, is shifted toward EG. No information about the reversibility of the reaction catalysed by *ADH1* and *GRE2* is available. GAH is further oxidized to GA by the action of nonspecific aldehyde dehydrogenases (*ALD2–6*, *ARI1*) using $NAD(P)^+$ as cofactor.

Process conditions optimization: DoE-aided biotransformation approach

Since *S. cerevisiae* showed the natural ability to oxidize EG to GA, we decided to develop a process for the production of GA. Carniel et al. (2023) developed a single-step process with *Y. lipolytica* for the production of GA from EG in YP medium. *Y. lipolytica*, indeed, is able to grow on YP efficiently and thus accumulate enough biomass for a viable conversion process. On the other hand, *S. cerevisiae* is not able to grow efficiently on YP alone, and addition of glucose in the medium to obtain the desired amount of biomass would cause a long delay in the oxidation of EG. Because of these reasons, we opted for a two-step bioconversion approach: first, biomass is produced on YPD in a 2-l bioreactor, then it is resuspended in the reaction mixture in lower volume (therefore at a higher concentration) in shake flasks. This approach also has the advantage of conducting the bioconversion in the desired buffer, as growth and production are separated; this aspect is very interesting when considering downstream purification, as less complex solutions can facilitate GA recovery.

Due to the lack of systematic information in literature about GA production from EG by yeast, a DoE approach was used to find the best bioconversion parameters for the second step of the process, to optimize production (final concentration of GA) and EG conversion; indeed, the use of an experimental design allows to evaluate the interaction among the variables, minimizing the experimental error and the number of experiments (Pagliari et al. 2022). The statistical model was developed in two stages: the first round had the objective to screen numerous parameters, to set up the base conditions and identify the factors that significantly influence EG conversion to GA; the second round was developed to refine the model using a lower number of factors, but with a better exploration of the response surface.

Results from Round 1

Nine different parameters were considered in the first round (see the section "Materials and methods"); shaking, m/f ratio and flask type were considered to study the effect of oxygenation and mass transfer; two EG concentrations and two reaction times (1 or 7 days) were tested. As previous experiments suggested that the EG oxidation machinery is expressed in late stationary phase (Fig. 1), we decided to test whether this aspect was crucial for this approach as well: thus, cells harvested during the exponential phase and cells in late stationary phase were compared for bioconversion efficiency; the initial amount of biomass for the bioconversion step was also taken into consideration. Finally, two different reaction media were tested: the rich medium YP and 100 mM potassium phosphate buffer. The effect of the initial pH was considered too, as the production of GA is expected to cause a decrease of the pH over time. Table S2 reports the experimental matrix design of Round 1, with the experimental levels of the selected parameters and the results obtained for the analysed response variables, GA concentration (g l^{-1}) and molar conversion of consumed EG to GA (% mol mol^{-1}). The statistical significance of the response variables is reported in Table S3. Medium composition resulted to be the most important factor, as it makes a positive contribution to both response variables. Shaking, growth phase and pH also showed a positive influence ($P < .05$) on conversion. Overall, the chemometric analysis suggested the following parameters in the optimized conditions: shaking (280 rpm), growth phase (stationary), medium (YP), pH (8), EG concentration (100 mM), m/f ratio (15), flask type (baffled), biomass (50 OD ml^{-1}), and time (7 days).

The results suggest that YP is a better reaction medium, probably because the nutrients present can sustain basal cell metabolism; moreover, YP also has a buffering capacity suggesting that higher and more stable pH can favor GA accumulation. Finally, the phase of growth in which cells are collected had a significant effect, suggesting that cells in late stationary phase might be preadapted and expressing the key genes for EG conversion. While the other variables did not show any significant effect, a trend can still be observed in the main effects plots (Fig. S2). Baffled shake flasks and higher m/f ratios increase mass transfer and oxygenation; a higher concentration of biomass improves the process, as well as a higher concentration of the reagent (EG); finally, the process proved to be relatively slow, with 7 days being the optimal bioconversion time.

Results from Round 2

For the next round of optimization, we decided to focus on shaking, medium composition and pH, while keeping the other parameters to the optimum conditions identified in the previous round. For the shaking, we decided to sample lower agitations to evaluate if a lower oxygenation would still allow for efficient EG conversion. While this aspect might be trivial at lab scale, it might cause issues when scaling up. In Round 1 the "medium" factor was designed as

a categorical variable: with the aim of reducing the amount of YP in the final product to facilitate GA purification, we transformed "medium" into a numerical variable, by considering different dilutions of the medium (1:1, 1:3, and 1:5). As pH cannot be increased above a certain threshold for toxicity reasons, we decided to dilute the YP medium with potassium phosphate buffer, and provide higher buffering capacity by modulating the concentration of the buffer (100, 200, or 300 mM); indeed, keeping a pH compatible with yeast growth and metabolism is key for an efficient process. Table 1 reports the experimental matrix design of Round 2, with the experimental levels of the independent variables (factors) and the results obtained for the analysed response variables, GA concentration (g l^{-1}) and molar conversion of consumed EG to GA (% mol mol^{-1}).

The statistical significance of the response variables studied can be observed from the standardized pareto chart for each experimental factor (Fig. 3). The significance of the effects at 95% confidence level is highlighted by the vertical line in the chart whereas positive (green) and negative (red) effects in the response variables were indicated by different bar colors. Shaking resulted to be the only significant factor for both response variables, suggesting once again the importance of an efficient oxygenation and mass transfer. This aspect was also hypothesized by Kataoka et al. (2001) and Carniel et al. (2023), who reported that oxygenation might be an issue in the bioconversion process; moreover, from a metabolic point of view, sufficient oxygenation might be necessary to regenerate the $NAD(P)^+$ required for EG oxidation in the electron transport chain according to the proposed pathway (Fig. 2).

Interestingly, dilution of the reaction medium YP and buffer concentration do not affect the response variables significantly, meaning that it is feasible to use the lowest concentration of buffer and a diluted medium to ease the purification process.

Overall, the chemometric analysis suggested the following parameters in the optimized conditions: shaking (280 rpm), YP dilution (1:1), and buffer concentration (100 mM), predicting 5.19 g l^{-1} of GA (3.48–6.94 g l^{-1}, 95% limits) and a conversion of 85.42% (68.10%–100.00%, 95% limits). It is worth mentioning that these optimized conditions refer specifically to *S. cerevisiae*, as other yeast species may respond differently.

The result was experimentally validated by performing the bioconversion in the optimized conditions, obtaining a production of 4.51 ± 0.12 g l^{-1} and a conversion of 94.25 ± 1.74%, reaching the optimum after only 4 days (Fig. S3). While we were not able to significantly increase the production with respect to other conditions (e.g. conditions 13, 14, and 15; see Table 1), we were able to increase the conversion to almost 95%, which is the highest conversion obtained in this set of experiments, and the productivity, reducing process time from 7 days to only 4 days. Most importantly, these results are in line with the ones predicted by the model, falling in the range of the predicted lower and upper bounds. Of note, we observed GA consumption after the peak of production (Fig. S3); to the best of our knowledge, this aspect has not been reported in literature: we speculate that GA might be consumed by further oxidation to GOX by *GOR1* (Rintala et al. 2007), with a NAD^+-dependent glyoxylate reductase activity usually reported to catalyse the reduction of GOX to GA (Koivistoinen et al. 2013, Salusjärvi et al. 2017). Indeed, no peaks relative to GAH or GOX were observed in the HPLC chromatograms, suggesting that GOX is metabolized through the glyoxilate cycle. Further studies are needed to confirm the role of *GOR1* and the destiny of GOX in the pathway.

Screening of yeast biodiversity for better GA-producing species

Screening of different yeast species

The results obtained with the bioconversion experiments were promising; however, *S. cerevisiae* showed different downsides, such as the inability to coconsume EG with glucose and the necessity of a two-step process, combined with the generally low biomass yield as it is a Crabtree-positive yeast, and the poor uptake of EG. For these reasons we decided to explore yeast biodiversity for better GA-producing strains, as well as to elucidate whether the ability to oxidize EG is a shared trait among yeasts. Indeed, only a few yeasts are reported to be able to metabolize EG, namely *Y. lipolytica*, *Pichia naganishii*, *Rhodotorula* sp., and *Hansenula sp.* (Carniel et al. 2024).

With this in mind, we screened nine yeasts in our library. In particular, among the phylum Ascomycota we considered *K. lactis*, the thermotolerant *K. marxianus*, the methylotrophic yeast *K. phaffii*, the robust *S. stipitis*, and the acid-tolerant yeasts *Z. bailii* and *Z. parabailii*. As many reports with the oleaginous yeast *Y. lipolytica* (Ascomycota) are available in literature, we decided to focus on oleaginous yeasts belonging to the phylum Basidiomycota and we included *C. oleaginosus* ATCC 20509, *C. oleaginosus* DSM 70022, and *R. toruloides*.

The ability to metabolize EG was evaluated in rich medium YP + EG 150 mM (9.3 g l^{-1}); as a control, *S. cerevisiae* was included in the experiment. The results are shown in Fig. 4. Interestingly, all the assayed yeast species not only were able to metabolize EG, but they were also all able to accumulate GA as a by-product. These results suggest that the ability to metabolize EG might be a common trait among yeasts, even from different phyla. Three yeast species stood out with particularly elevated GA productions: *K. phaffii* produced 76.7 ± 0.4 mM (5.83 ± 0.03 g l^{-1}), *C. oleaginosus* ATCC 20509 produced 83.0 ± 1.1 mM (6.31 ± 0.08 g l^{-1}), and *S. stipitis* produced 112.0 ± 0.4 mM (8.53 ± 0.03 g l^{-1}); in comparison, *S. cerevisiae* was only able to produce 34.2 ± 0.8 mM (2.60 ± 0.06 g l^{-1}) of GA in these conditions. From these preliminary results, we decided to better characterize GA production with the top two performers. It is worth mentioning that *K. phaffii* remains a very interesting yeast for the oxidation of EG: indeed, an *in vitro* study (Isobe and Nishise 1994) demonstrated that the alcohol oxidase *AOX1* is able to oxidize EG to GAH (and GAH to the undesired product glyoxal) in a nonreversible way. Thus, addition of methanol to strongly induce *AOX1* might improve EG conversion to GA.

Characterization of GA production by S. stipitis and C. oleaginosus ATCC 20509

To better understand EG metabolism by *S. stipitis* and *C. oleaginosus* ATCC 20509, the two yeasts were grown in YP + EG in 6-deepwell microplates; as a control, the yeasts were also grown in YP without the addition of EG. To account for the drop in pH due to the production of GA, the medium was buffered to pH 7. Enzyscreen microplates were selected as they guarantee high oxygenation of the cultures (30–40 mmol O_2 l^{-1} h^{-1}) while also limiting the evaporation (enzyscreen.com), as oxygenation and mass transfer revealed to be the key parameter in the bioconversion experiments with *S. cerevisiae*.

The presence of EG did not cause any differences in the growth of the two yeasts, which showed the same maximum specific growth rate with the control condition (0.28 ± 0.01 h^{-1} and 0.26 ± 0.02 h^{-1} for *S. stipitis*, and 0.37 ± 0.05 h^{-1} and 0.36 ± 0.05 h^{-1} for *C. oleaginosus*) (Fig. 5C).

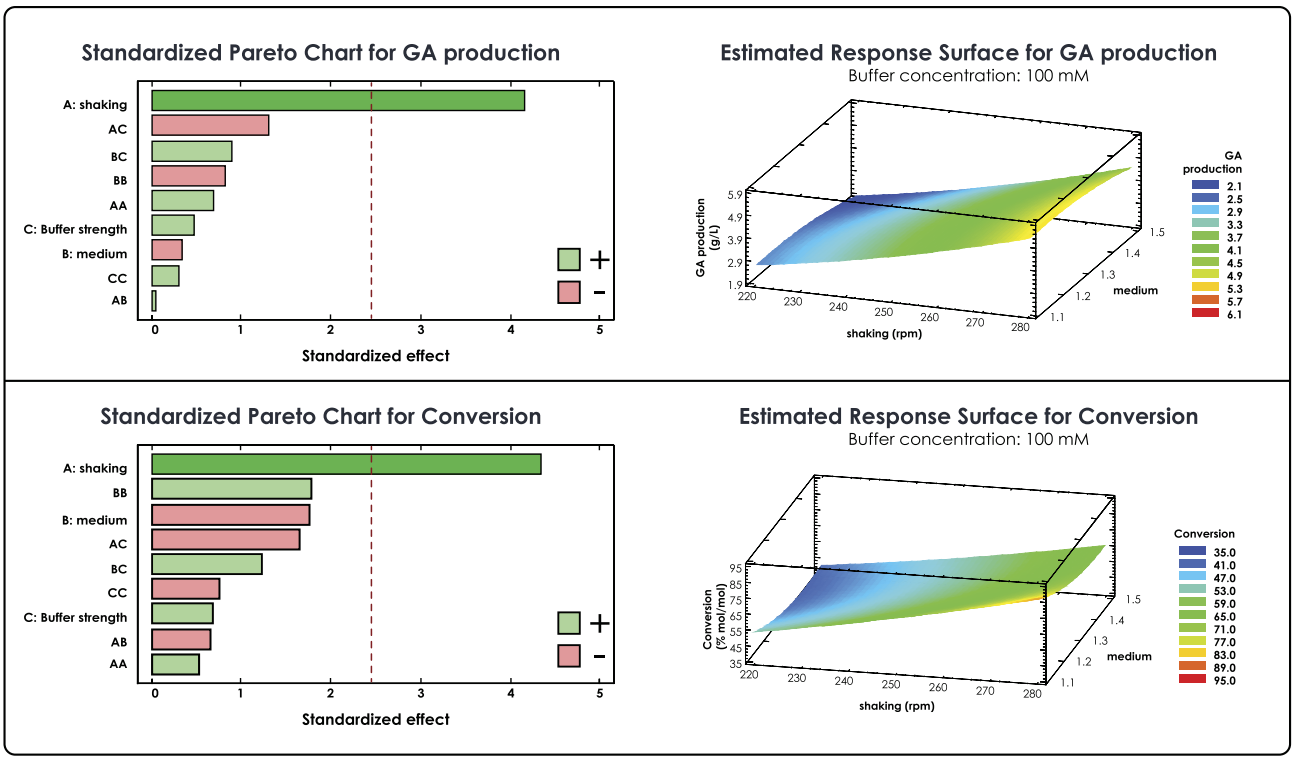

Figure 3. Standardized Pareto Charts and Estimated Response Surfaces for GA production (top) and Conversion (bottom) from Round 2. The standardized Pareto Charts show the estimated positive (green) and negative (red) effects of each term in the Box–Behnken design model in decreasing order of significance. Bars beyond the red vertical line are statistically significant with a confidence level of 95%. The Estimated Response Surface plots represent the predicted value of GA production (g l^{-1}) and Conversion (% mol mol^{-1}) over the space of shaking (220–280 rpm) and medium (1.1–1.5); buffer concentration was held constant at 100 mM, which is the value in the optimized condition.

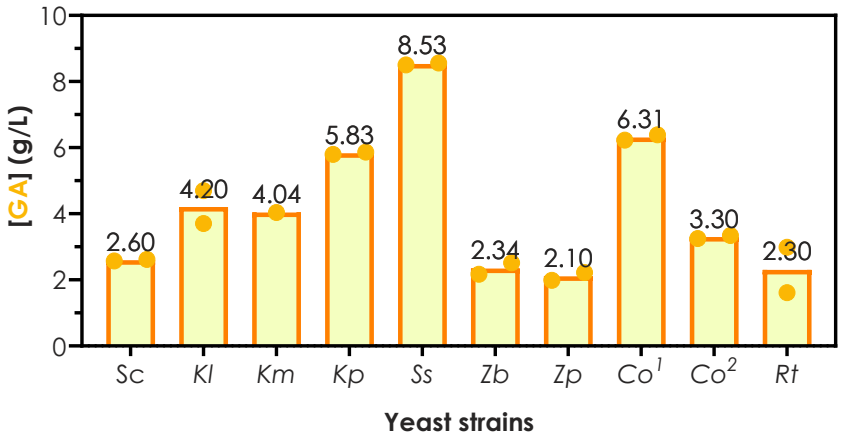

Figure 4. GA production from EG by non-*Saccharomyces* yeasts. Bars are the mean of two independent experiments; the value of each replicate is represented by a circle; the value of the mean is expressed on top of the bars. Sc, *S. cerevisiae*; Kl, *K. lactis*; Km, *K. marxianus*; Kp, *K. phaffii*; Ss, *S. stipitis*; Zb, *Z. bailii*; Zp, *Z. parabailii*; Co^1, *C. oleaginosus* (ATCC 20509); Co^2, *C. oleaginosus* (DSM 70022); and Rt, *R. toruloides*.

In the case of *S. stipitis*, EG consumption and GA production most probably start at the beginning of the fermentation; however, quantification of GA was possible only from 6 h. The production of GA shows a linear trend, slowing down towards the end of the fermentation (56 h). The slower rate might be due to the decrease of the pH to 5 (Fig. 5A). In the case of *C. oleaginosus*, two distinct phases of EG consumption and GA production can be observed. Initially (0–24 h), EG consumption is slow; between 24 and 72 h, a faster rate is observed, resulting in the maximum GA production at 72 h. Interestingly, a third phase is observed between 72 and 144 h, where EG and GA are coconsumed; no by-products could be observed in the chromatograms (Fig. 5B). *Scheffersomyces stipitis* and *C. oleaginosus* seem to behave differently with respect to EG conversion. Moreover, their behavior is also different from what Carniel et al. (2023) reported for *Y. lipolytica* grown in similar conditions. *Y. lipolytica* shows an initial fast consumption of EG related to a low GA production; a second phase is characterized by a lower consumption rate of EG, however, related to a higher GA production rate. No GA consumption was observed.

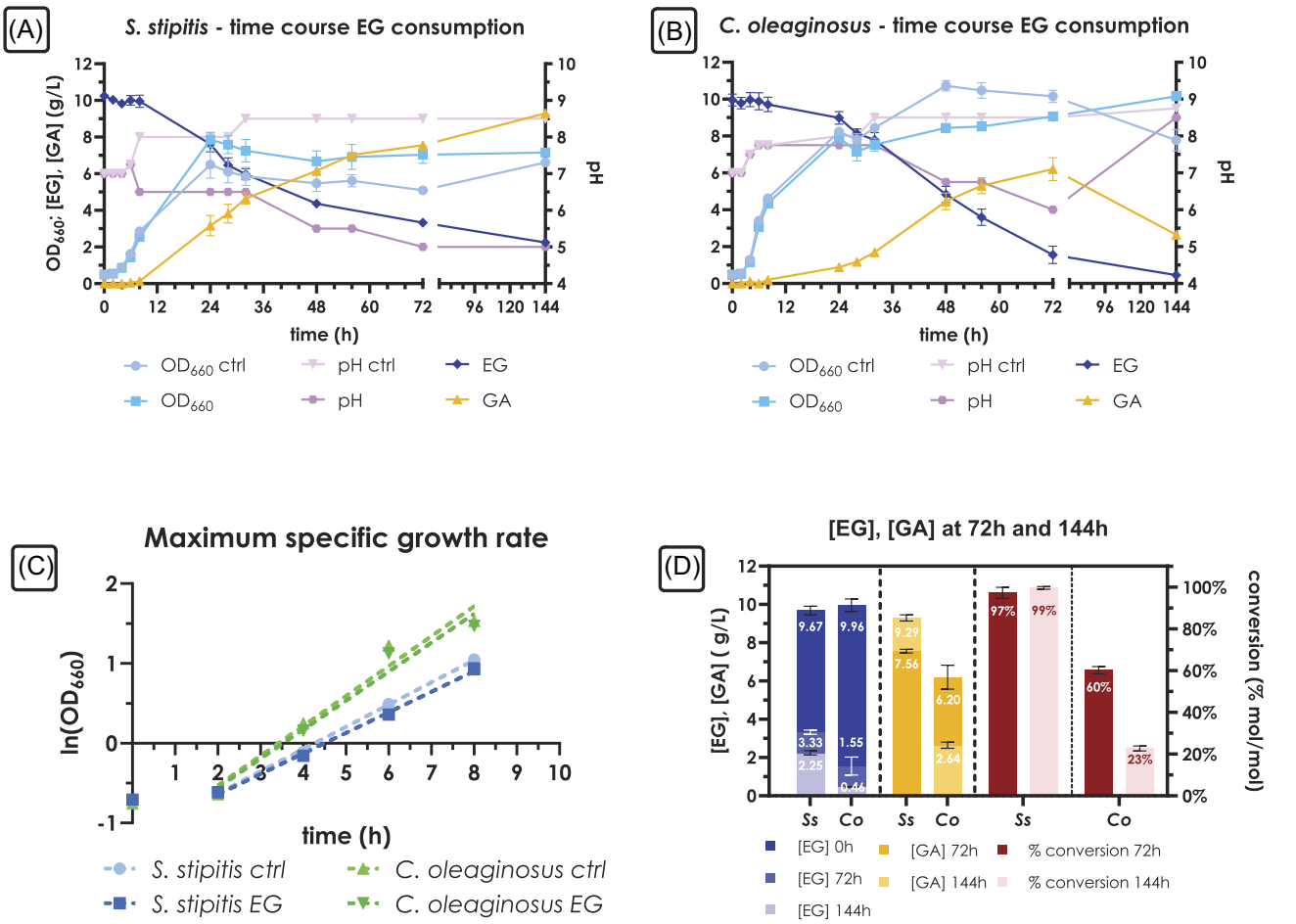

Figure 5. Fermentation profiles, growth rate, and GA production by *S. stipitis* and *C. oleaginosus* (ATCC 20509) in 6-deepwell microplates. Panels (A) and (B) show the fermentation profiles of *S. stipitis* and *C. oleaginosus*, respectively; lighter shades of the color refer to the control conditions. Panel (C) shows the maximum specific growth rate in the exponential phase for *S. stipitis* and *C. oleaginosus*; lighter shades of the color refer to the control conditions. Panel (D) shows EG consumption, GA production and conversion at 72 h and 144 h for *S. stipitis* (*Ss*) and *C. oleaginosus* (*Co*). The left *y*-axis shows EG at the beginning of the fermentation (dark blue bars), EG at 72 h (blue bars) and GA at 72 h (dark yellow bars), and EG at 144 h (light blue bars) and GA at 144 h (light yellow bars), in g l^{-1}; the right *y*-axis shows EG conversion into GA at 72 h (dark red bars) and 144 h (light red bars); the percentage is expressed on the consumed EG; the value of the means is expressed inside each bar. *Ss*, *S. stipitis*; *Co*, *C. oleaginosus* (ATCC 20509). Values are the mean ± standard deviation of three independent experiments.

The highest GA production was obtained with *S. stipitis*, reaching 122.0 ± 1.7 mM (9.29 ± 0.13 g l^{-1}) after 144 h, with a conversion yield of the consumed EG of 99%. This suggests that *S. stipitis* does not readily consume GA after the production. *C. oleaginosus* produced 81.5 ± 6.7 mM (6.20 ± 0.51 g l^{-1}) after 72 h, with a conversion around 60%, suggesting that 40% of the consumed EG is metabolized either via another pathway, or further oxidized to GOX, as suggested for *S. cerevisiae*. The results are summarized in Fig. 5(D). Compared with the results obtained in the bioconversion experiment with *S. cerevisiae*, both yeasts were able to produce a higher amount of GA, in a much simpler process with a relatively low cell density, with *S. stipitis* producing twice as much as *S. cerevisiae*, with a higher conversion rate. Because of this, *S. stipitis* was selected for the process scale-up to 2 l bioreactors.

Production of GA with S. stipitis in 2 l bioreactors

Given the promising results from the previous experiments, GA production was evaluated with *S. stipitis* in stirred tank reactors. The process starts with biomass accumulation; after the exhaustion of the carbon source, EG is added for the conversion. As sometimes working with defined media with *S. stipitis* is tricky (Mastella et al. 2022) and to maximize biomass yield, we decided to grow the yeast on YPD, with 40 g l^{-1} of glucose. This approach also ensured a similar medium composition (YP) as in the previous experiments, at the time of addition of EG at the end of growth phase (24 h).

Scheffersomyces stipitis was able to completely convert 11 ml of EG (197 mmol, 250 mM, and 12.2 g) into 151 mmol (11.5 g) of GA; all the EG was consumed (100% consumption), and the yield of GA (% mol mol^{-1}) accounting for volume loss due to evaporation during fermentation was 76.68%. The concentration of GA in the supernatant was 313 ± 16 mM (23.79 ± 1.19 g l^{-1}), with a productivity of 190.41 mg_{GA} l^{-1} h^{-1}. Figure 6 shows the fermentation profile and process statistics.

It is interesting to note that over the time of EG consumption, about 80 mmol of CO_2 were produced; considering that about 46 mmol of EG were not converted to GA, we can estimate the amount of CO_2 that would be produced if EG was completely oxidized, e.g. by conversion to GOX and further oxidation to CO_2 via the TCA cycle; this process would produce 2 moles of CO_2 for every mole of EG (Franden et al. 2018), for a total of 92 mmol of CO_2, which is particularly close to the measured experimental value. These results suggest that EG

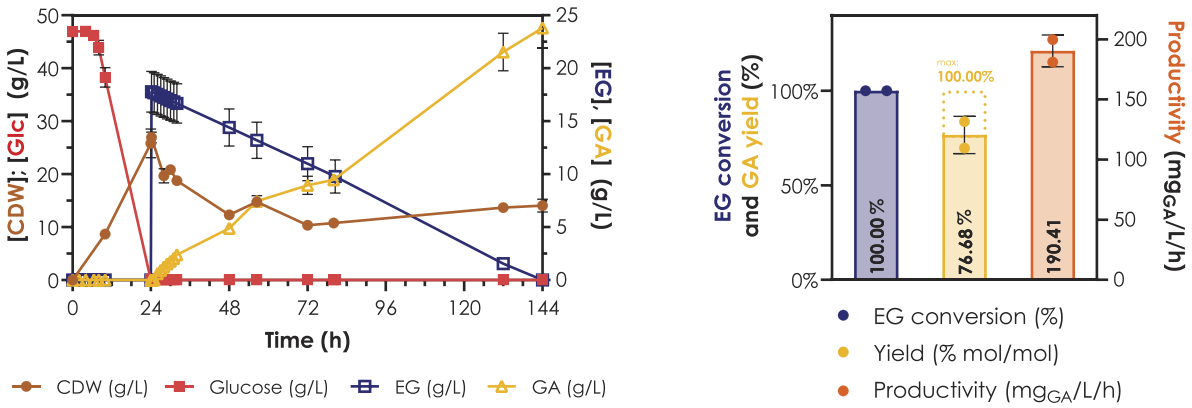

Figure 6. Fermentation profile and process statistics of GA production from EG in 2 l bioreactors by *S. stipitis*. The left panel shows the fermentation profile of *S. stipitis*; the left *y*-axis shows CDW (brown, circles), and glucose (red, squares), concentration in g l^{-1}; the right *y*-axis shows EG (dark blue, hollow squares) and GA (yellow, hollow triangles) concentration in g l^{-1}. The right panel shows EG conversion, yield of GA (left *y*-axis), and productivity (right *y*-axis). Values are the mean ± standard error of two independent experiments.

is oxidized completely to GA; however, a small fraction of it might be further metabolized to GOX and ultimately respired to CO_2. More in depth studies are needed to confirm this aspect.

For the economics of the process, it must be noted that glucose is required to obtain the initial biomass. As a proof of concept, we utilized pure glucose, however, *S. stipitis* is a robust microbial cell factory capable of utilizing both C6 and C5 sugars (Mastella et al. 2022). Thus, a lignocellulose-derived growth medium could be used to produce the biomass in a more sustainable way; moreover, the presence of other sugars and nutrients might improve EG conversion to GA, sustaining growth during the production phase. More studies are needed to improve the proposed process: as an example, one of the main points would be to understand if C5 sugars inhibit EG oxidation as glucose does.

Finally, the goal was also to develop a process, which did not rely on offline data. Growth and glucose consumption phase can be estimated by the online profile of the pO_2, clearly indicating the time of addition of EG. Moreover, as GA is the only by-product, by separating growth and production phase it is possible to monitor the conversion of EG to GA by the addition of base, without requiring any special equipment (e.g. HPLC). To confirm that this was possible, we estimated the final amount of GA based on the volume of added KOH and compared it to the actual value. At the end of EG consumption, 86 ml of base had been added after the addition of EG, and using Equation (1), an estimate of 13 g of GA was obtained; this value is close to the value measured by HPLC at the end of the fermentation (11.5 g). We conclude that the base profile can be used for online monitoring of GA production from EG. Figure S4 shows a visual representation of the process monitoring described above.

Taken together, our findings reveal yeasts as an interesting biorefinery for the upcycling of EG to GA. To the best of our knowledge, only two other works studied EG conversion to GA by yeast. Carniel et al. (2023) obtained similar results to ours; they were able to obtain 429 mM (32.6 g l^{-1}) of GA with a yield on consumed EG of 74% (35% when considering total EG) by growing *Y. lipolytica* in YP + EG 1 M in a bioreactor setting; Kataoka et al. (2001) were able to obtain up to 1.45 M (110 g l^{-1}) with a yield of 92% by growing *Rhodotorula* sp. in high density bioconversions (10.7 g of wet cell weight for a 100 ml reaction).

Conclusions

The scope of this work was to lay the foundations to study the physiology of EG metabolism in different yeasts, as their specific metabolic traits can offer advantages in different process conditions and with different media compositions.

Firstly, we demonstrated that EG consumption in *S. cerevisiae* growing in the presence of glucose only starts after the depletion of other carbon sources (glucose, acetate, and ethanol), unlike what happens in *Y. lipolytica*; a DoE approach allowed to pinpoint the most important parameters to optimize a two-step bioconversion and to develop a predictive model for *S. cerevisiae*; moreover, a putative pathway for the metabolism of EG by *S. cerevisiae* was proposed. Secondly, screening of ascomycete and basidiomycete yeasts revealed that the ability to oxidize EG to GA is a pretty common trait among yeasts. Since EG is not generally found in their natural niches, yeasts most likely did not evolve specific enzymes active on this molecule. From a structural point of view, EG can be associated to 1,2-propanediol (as often reported for bacteria), or most likely ethanol or glycerol; therefore, we can speculate that oxidation of EG is catalysed by promiscuous endogenous alcohol dehydrogenases evolved for other (poly)alcohols.

Further studies are required to better understand the genes and metabolic pathways involved in EG oxidation, including deletion and/or overexpression of the identified genes; precision editing *in S. cerevisiae* can confirm or deny our initial hypotheses. In parallel, further efforts might be directed to the identification of more performing yeast species, or strains with different EG consumption strategies.

One last remark should be made about the economic feasibility of the process. Indeed, the added value generated by conversion of EG to GA might not be sufficient to cover the cost of a process encompassing the enzymatic hydrolysis of PET and the subsequent production of GA. Most probably, yield and productivity will need to be improved, together with the identification of a more economic substrate for the growth of *S. stipitis* and a viable GA purification system. However, it must be taken into consideration that the TPA released by the PET hydrolysis can also be converted by bacteria to the much more valuable protocatechuic acid, as many examples are present in literature. Taken together, a techno-economic analysis will be necessary to understand the feasibility of such a complex process.

Acknowledgements

We thank Ilaria Spreafico and Monica Squicciarini for their help in the bioconversion experiments.

Supplementary data

Supplementary data is available at *FEMSYR Journal* online.

Conflict of interest : None declared.

Funding

This work was supported by the European Union's Horizon 2020 research and innovation programme under grant agreement number 101036838, by Ministero dell'Istruzione e del Merito (MIUR) PRIN number 2020SBNHLH, and by the European COST programme, Action N° CA18229 Yeast4Bio (Non-Conventional Yeasts for the Production of Bioproducts).

References

Amalia L, Chang C-Y, Wang SS-S *et al.* Recent advances in the biological depolymerization and upcycling of polyethylene terephthalate. *Curr Opin Biotechnol* 2024;**85**:103053. https://doi.org/10.1016/j.copbio.2023.103053.

Cabulong RB, Valdehuesa KNG, Bañares AB *et al.* Improved cell growth and biosynthesis of glycolic acid by overexpression of membrane-bound pyridine nucleotide transhydrogenase. *J Ind Microbiol Biotechnol* 2019;**46**:159–69. https://doi.org/10.1007/s10295-018-2117-2.

Carbios. CARBIOS Corporate Presentation. Clermont-Ferrand, 2024. https://www.carbios.com/wp-content/uploads/2022/01/carbios_presentation-january-2022.pdf (25 April 2024, date last accessed).

Carniel A, Santos AG, Chinelatto LS *et al.* Biotransformation of ethylene glycol to glycolic acid by *Yarrowia lipolytica*: a route for poly(ethylene terephthalate) (PET) upcycling. *Biotechnol J* 2023;**18**:2200521. https://doi.org/10.1002/biot.202200521.

Carniel A, Santos NFd, Buarque FS *et al.* From trash to cash: current strategies for bio-upcycling of recaptured monomeric building blocks from poly(ethylene terephthalate) (PET) waste. *Green Chem* 2024;**6**:5708–43, https://doi.org/10.1039/D4GC00528G.

Da Costa AM, De Oliveira Lopes VR, Vidal L *et al.* Poly(ethylene terephthalate) (PET) degradation by *Yarrowia lipolytica*: investigations on cell growth, enzyme production and monomers consumption. *Process Biochem* 2020;**95**:81–90. https://doi.org/10.1016/j.procbio.2020.04.001.

Deng Y, Ma N, Zhu K *et al.* Balancing the carbon flux distributions between the TCA cycle and glyoxylate shunt to produce glycolate at high yield and titer in *Escherichia coli*. *Metab Eng* 2018;**46**:28–34. https://doi.org/10.1016/j.ymben.2018.02.008.

Franden MA, Jayakody LN, Li W-J *et al.* Engineering *Pseudomonas putida* KT2440 for efficient ethylene glycol utilization. *Metab Eng* 2018;**48**:197–207. https://doi.org/10.1016/j.ymben.2018.06.003.

Gao R, Pan H, Kai L *et al.* Microbial degradation and valorization of poly(ethylene terephthalate) (PET) monomers. *World J Microbiol Biotechnol* 2022;**38**:89. https://doi.org/10.1007/s11274-022-03270-z.

Hua X, Cao R, Zhou X *et al.* Integrated process for scalable bioproduction of glycolic acid from cell catalysis of ethylene glycol. *Bioresour Technol* 2018;**268**:402–7. https://doi.org/10.1016/j.biortech.2018.08.021.

Hundertmark T, Mayer M, McNally C *et al. How Plastics-Waste Recycling Could Transform the Chemical Industry*. New York: McKinsey & Company, 2018. https://www.mckinsey.com/~/media/McKinsey/Industries/Chemicals/Our%20Insights/How%20plastics%20waste%20recycling%20could%20transform%20the%20chemical%20industry/How-plastics-waste-recycling-could-transform.pdf (25 April 2024, date last accessed).

Isobe K, Nishise H. Enzymatic production of glyoxal from ethylene glycol using alcohol oxidase from methanol yeast. *Biosci Biotechnol Biochem* 1994;**58**:170–3. https://doi.org/10.1271/bbb.58.170.

Jayakody LN, Horie K, Hayashi N *et al.* Engineering redox cofactor utilization for detoxification of glycolaldehyde, a key inhibitor of bioethanol production, in yeast *Saccharomyces cerevisiae*. *Appl Microbiol Biotechnol* 2013;**97**:6589–600. https://doi.org/10.1007/s00253-013-4997-4.

Jayakody LN, Jin Y-S. In-depth understanding of molecular mechanisms of aldehyde toxicity to engineer robust *Saccharomyces cerevisiae*. *Appl Microbiol Biotechnol* 2021;**105**:2675–92. https://doi.org/10.1007/s00253-021-11213-1.

Jayakody LN, Turner TL, Yun EJ *et al.* Expression of *Gre2p* improves tolerance of engineered xylose-fermenting *Saccharomyces cerevisiae* to glycolaldehyde under xylose metabolism. *Appl Microbiol Biotechnol* 2018;**102**:8121–33. https://doi.org/10.1007/s00253-018-9216-x.

Kataoka M, Sasaki M, Hidalgo A-RGD *et al.* Glycolic acid production using ethylene glycol-oxidizing microorganisms. *Biosci Biotechnol Biochem* 2001;**65**:2265–70. https://doi.org/10.1271/bbb.65.2265.

Koivistoinen OM, Kuivanen J, Barth D *et al.* Glycolic acid production in the engineered yeasts *Saccharomyces cerevisiae* and *Kluyveromyces lactis*. *Microb Cell Fact* 2013;**12**:82. https://doi.org/10.1186/1475-2859-12-82.

Kosiorowska KE, Biniarz P, Dobrowolski A *et al.* Metabolic engineering of *Yarrowia lipolytica* for poly(ethylene terephthalate) degradation. *Sci Total Environ* 2022a;**831**:154841. https://doi.org/10.1016/j.scitotenv.2022.154841.

Kosiorowska KE, Moreno AD, Iglesias R *et al.* Production of PETase by engineered *Yarrowia lipolytica* for efficient poly(ethylene terephthalate) biodegradation. *Sci Total Environ* 2022b;**846**:157358. https://doi.org/10.1016/j.scitotenv.2022.157358.

Lee S, Lee YR, Kim SJ *et al.* Recent advances and challenges in the biotechnological upcycling of plastic wastes for constructing a circular bioeconomy. *Chem Eng J* 2023;**454**:140470. https://doi.org/10.1016/j.cej.2022.140470.

Levin BJ, Balskus EP. Characterization of 1,2-propanediol dehydratases reveals distinct mechanisms for B $_{12}$-dependent and glycyl radical enzymes. *Biochemistry* 2018;**57**:3222–6. https://doi.org/10.1021/acs.biochem.8b00164.

Mastella L, Senatore VG, Guzzetti L *et al.* First report on Vitamin B9 production including quantitative analysis of its vitamers in the yeast *Scheffersomyces stipitis*. *Biotechnol Biofuels* 2022;**15**:98. https://doi.org/10.1186/s13068-022-02194-y.

Muringayil Joseph T, Azat S, Ahmadi Z *et al.* Polyethylene terephthalate (PET) recycling: a review. *Case Stud Chem Environ Eng* 2024;**9**:100673. https://doi.org/10.1016/j.cscee.2024.100673.

Orlando M, Molla G, Castellani P *et al.* Microbial enzyme biotechnology to reach plastic waste circularity: current status, problems and perspectives. *Int J Mol Sci* 2023;**24**:3877. https://doi.org/10.3390/ijms24043877.

Pagliari S, Celano R, Rastrelli L *et al.* Extraction of methylxanthines by pressurized hot water extraction from cocoa shell by-product as natural source of functional ingredient. *LWT* 2022;**170**:114115. https://doi.org/10.1016/j.lwt.2022.114115.

Ren T, Zhan H, Xu H *et al.* Recycling and high-value utilization of polyethylene terephthalate wastes: a review. *Environ Res* 2024;**249**:118428. https://doi.org/10.1016/j.envres.2024.118428.

Rintala E, Pitkänen J, Vehkomäki M *et al.* The ORF *YNL274c* (*GOR1*) codes for glyoxylate reductase in *Saccharomyces cerevisiae*. *Yeast* 2007;**24**:129–36. https://doi.org/10.1002/yea.1434.

Sales JCS, Botelho AM, Carvalho ASS *et al.* Evaluation of *Yarrowia lipolytica* potential for the biodegradation of poly(ethylene terephthalate) (PET) from mooring lines of oil & gas offshore platforms. *Clean Chem Eng* 2023;**7**:100109. https://doi.org/10.1016/j.clce.2023.100109

Sales JCS, De Castro AM, Ribeiro BD *et al.* Post-consumer poly(ethylene terephthalate) (PET) depolymerization by *Yarrowia lipolytica*: a comparison between hydrolysis using cell-free enzymatic extracts and microbial submerged cultivation. *Molecules* 2022;**27**:7502. https://doi.org/10.3390/molecules27217502.

Salusjärvi L, Havukainen S, Koivistoinen O *et al.* Biotechnological production of glycolic acid and ethylene glycol: current state and perspectives. *Appl Microbiol Biotechnol* 2019;**103**:2525–35. https://doi.org/10.1007/s00253-019-09640-2.

Salusjärvi L, Toivari M, Vehkomäki M-L *et al.* Production of ethylene glycol or glycolic acid from D-xylose in *Saccharomyces cerevisiae*. *Appl Microbiol Biotechnol* 2017;**101**:8151–63. https://doi.org/10.1007/s00253-017-8547-3.

Soong Y-HV, Sobkowicz MJ, Xie D. Recent advances in biological recycling of polyethylene terephthalate (PET) plastic wastes. *Bioeng* 2022;**9**:98. https://doi.org/10.3390/bioengineering9030098.

Tiso T, Winter B, Wei R *et al.* The metabolic potential of plastics as biotechnological carbon sources—review and targets for the future. *Metab Eng* 2022;**71**:77–98. https://doi.org/10.1016/j.ymben.2021.12.006.

Tournier V, Topham CM, Gilles A *et al.* An engineered PET depolymerase to break down and recycle plastic bottles. *Nature* 2020;**580**:216–9. https://doi.org/10.1038/s41586-020-2149-4.

Trifunović D, Schuchmann K, Müller V. Ethylene glycol metabolism in the acetogen *Acetobacterium woodii*. *J Bacteriol* 2016;**198**:1058–65. https://doi.org/10.1128/JB.00942-15.

Verduyn C, Postma E, Scheffers WA *et al.* Effect of benzoic acid on metabolic fluxes in yeasts: a continuous-culture study on the regulation of respiration and alcoholic fermentation. *Yeast* 1992;**8**:501–17. https://doi.org/10.1002/yea.320080703.

Wang H, Li Q, Zhang Z *et al.* YKL107W from *Saccharomyces cerevisiae* encodes a novel aldehyde reductase for detoxification of acetaldehyde, glycolaldehyde, and furfural. *Appl Microbiol Biotechnol* 2019;**103**:5699–713. https://doi.org/10.1007/s00253-019-09885-x.

Wang H-Y, Xiao D-F, Zhou C *et al.* YLL056C from *Saccharomyces cerevisiae* encodes a novel protein with aldehyde reductase activity. *Appl Microbiol Biotechnol* 2017;**101**:4507–20. https://doi.org/10.1007/s00253-017-8209-5.

Weiland F, Kohlstedt M, Wittmann C. Biobased de novo synthesis, upcycling, and recycling—the heartbeat toward a green and sustainable polyethylene terephthalate industry. *Curr Opin Biotechnol* 2024;**86**:103079. https://doi.org/10.1016/j.copbio.2024.103079.

Yu Q, Liu X, Lv Y *et al.* Tandem production of high-purity sodium glycolate via the dual purification technology of crystallization and active carbon adsorption. *Chem Eng J* 2023;**452**:138994. https://doi.org/10.1016/j.cej.2022.138994.

Zhang X, Zhang B, Lin J *et al.* Oxidation of ethylene glycol to glycolaldehyde using a highly selective alcohol dehydrogenase from *Gluconobacter oxydans*. *J Mol Catal B Enzym* 2015;**112**:69–75. https://doi.org/10.1016/j.molcatb.2014.12.006.

Received 17 June 2024; **revised** 26 July 2024; **accepted** 2 August 2024